

Recent Advances in Adaptive Radar Detection

Maria Greco¹, Frédéric Pascal², Jean-Philippe Ovarlez^{2,3}

¹Pisa University, Italy

²E3S-SONDRA, Supélec, France

³French Aerospace Lab, ONERA DEMR/TSI, France

Radar Conference 2014
October 2014

Contents

- **Part A** Done
Background on Clutter Modeling and Modern Radar Detection
- **Part B** Done
Adaptive Detection and Covariance Matrix Estimation
- **Part C**
Radar Applications

Part C

Radar Applications

Part C: Contents

- 1 More properties of the adaptive detectors
 - Robustness of the M-estimators
 - Adaptive Robust Detection in Clutter Transition
 - Exploiting Prior Information: Covariance Structure
 - Low Rank Detectors
- 2 Radar applications: Doppler detection/estimation, STAP
 - Surveillance Radar Data
 - OTH Radar Data
 - STAP Data
- 3 Conclusions and Perspectives

Outline

1 More properties of the adaptive detectors

■ Robustness of the M-estimators

■ Adaptive Robust Detection in Clutter Transition

■ Exploiting Prior Information: Covariance Structure

■ Low Rank Detectors

2 Radar applications: Doppler detection/estimation, STAP

■ Surveillance Radar Data

■ OTH Radar Data

■ STAP Data

3 Conclusions and Perspectives

Robustness of the M-estimators

Let us suppose that $\{\mathbf{c}_i\}_{i=1,K-1} \sim \mathcal{CN}(\mathbf{0}, \mathbf{M})$ and the last secondary data \mathbf{c}_K contains outlier \mathbf{p}_0 :

- Sample Covariance Matrix case:

$$\hat{\mathbf{M}}_{SCM}^{pol} = \frac{1}{K} \sum_{k=1}^{K-1} \mathbf{c}_k \mathbf{c}_k^H + \frac{1}{K} \mathbf{p}_0 \mathbf{p}_0^H \quad E \left[\hat{\mathbf{M}}_{SCM}^{pol} \right] = \frac{K-1}{K} \mathbf{M} + \frac{1}{K} E \left[\mathbf{p}_0 \mathbf{p}_0^H \right]$$

The power of the outlier \mathbf{p}_0 has a **big impact** on the quality of the SCM estimation

- Tyler (or FP) Covariance Matrix case:

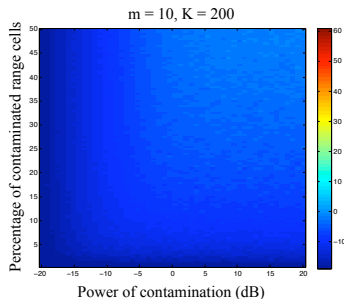
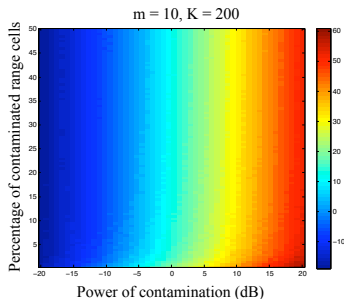
$$\hat{\mathbf{M}}_{FPpol} = \frac{m}{K} \sum_{k=1}^K \frac{\mathbf{c}_k \mathbf{c}_k^H}{\mathbf{c}_k^H \hat{\mathbf{M}}_{FPpol}^{-1} \mathbf{c}_k} \quad E \left[\hat{\mathbf{M}}_{FPpol} \right] = \mathbf{M} + \frac{m+1}{K} \left[E \left[\frac{\mathbf{p}_0 \mathbf{p}_0^H}{\mathbf{p}_0^H \mathbf{M}^{-1} \mathbf{p}_0} \right] - \frac{1}{m} \mathbf{M} \right]$$

The power of the outlier \mathbf{p}_0 has **no big impact** on the quality of the Tyler estimate

Robustness of the M-estimators

Gaussian vectors \mathbf{c}_k polluted by outliers

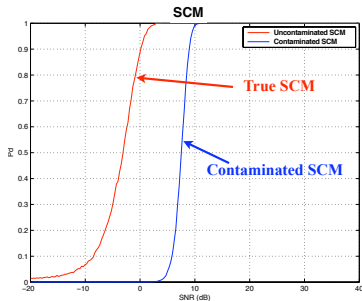
$$\hat{\mathbf{M}}_{SCM} = \frac{1}{K} \sum_{k=1}^K \mathbf{c}_i \mathbf{c}_k^H \quad \hat{\mathbf{M}}_{FP} = \frac{m}{K} \sum_{k=1}^K \frac{\mathbf{c}_k \mathbf{c}_k^H}{\mathbf{c}_k^H \hat{\mathbf{M}}_{FP}^{-1} \mathbf{c}_k}$$



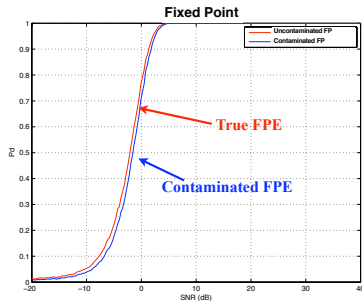
Plot of the error between the covariance matrix estimated with and without outliers

Potential Impact on detection performance

Same target c_k (SNR 20dB) than those in the cell under test
in the reference cells



AMF + SCM



ANMF + FPE

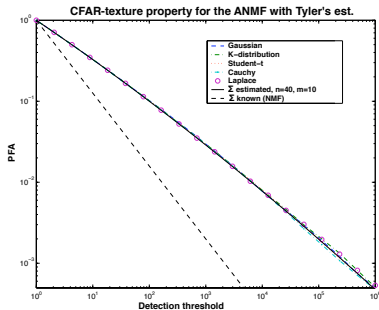
The SCM can whiten the target to detect
The FPE is more robust
(case of convoy for example)

Outline

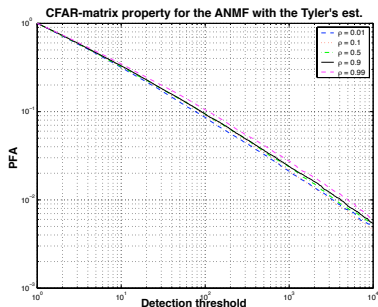
- 1 More properties of the adaptive detectors
 - Robustness of the M-estimators
 - Adaptive Robust Detection in Clutter Transition
 - Exploiting Prior Information: Covariance Structure
 - Low Rank Detectors
- 2 Radar applications: Doppler detection/estimation, STAP
 - Surveillance Radar Data
 - OTH Radar Data
 - STAP Data
- 3 Conclusions and Perspectives

SIRV-CFAR Properties of ANMF-Tyler Detector in heterogeneous clutter

False Alarm regulation



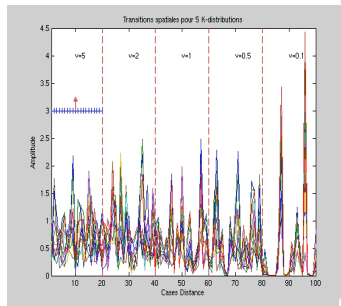
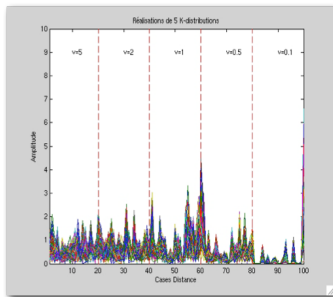
(a) CFAR-texture



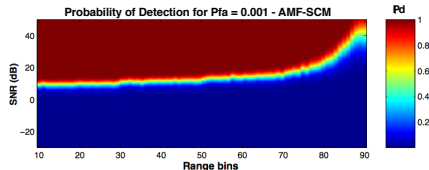
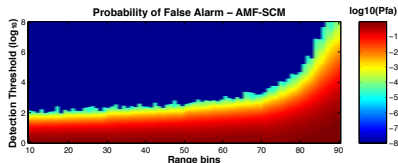
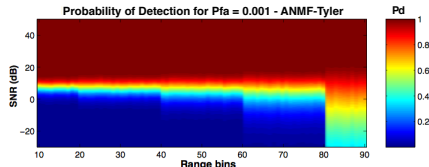
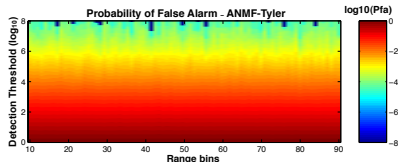
(b) CFAR-matrix

Figure: Illustration of the CFAR properties of the ANMF built with the Tyler's estimator, for a Toeplitz CM whose (i, j) -entries are $\rho^{|i-j|}$

Properties of ANMF-Tyler Detector on Clutter Statistic Transitions



- K-distributed clutter transitions: from Gaussian to impulsive noise
- Estimation of the covariance matrix onto a range bins sliding window



- ANMF-Tyler: The same detection threshold is guaranteed for a chosen P_{fa} whatever the clutter area
- ANMF-Tyler: Performance in term of detection is kept for moderate non-Gaussian clutter and improved for spiky clutter

Outline

1 More properties of the adaptive detectors

- Robustness of the M-estimators
- Adaptive Robust Detection in Clutter Transition
- Exploiting Prior Information: Covariance Structure
- Low Rank Detectors

2 Radar applications: Doppler detection/estimation, STAP

- Surveillance Radar Data
- OTH Radar Data
- STAP Data

3 Conclusions and Perspectives

Motivations

The estimation of \mathbf{M} does not take into account any prior knowledge on the covariance matrix:

How to improve detection performance by exploiting prior information on \mathbf{M} ?

⇒ Use of some prior knowledge on the structure of the covariance matrix:

- Toeplitz: Burg [82] for estimation, Fuhmann [91] for detection in Gaussian case,
- known rank $r < m$ (ex: subspace detector),
- **Persymmetry**: Nitzberg [80] for estimation, Kai-Wang [92] for detection in Gaussian case, Conte and De Maio [03, 04], Pailloux *et al.* [10] in non-Gaussian noise.

Using Persymmetry Property

Under persymmetric considerations (ex: symmetrically spaced linear array, symmetrically spaced pulse train, ...), the Hermitian covariance matrix \mathbf{M} verifies: $\mathbf{M} = \mathbf{J}_m \mathbf{M}^* \mathbf{J}_m$, where \mathbf{J}_m is the m -dimensional antidiagonal matrix having 1 as non-zero elements. If the unitary matrix \mathbf{T} is defined by:

$$\mathbf{T} = \begin{cases} \frac{1}{\sqrt{2}} \begin{pmatrix} \mathbf{I}_{m/2} & \mathbf{J}_{m/2} \\ i \mathbf{I}_{m/2} & -i \mathbf{J}_{m/2} \end{pmatrix} & \text{for } m \text{ even} \\ \frac{1}{\sqrt{2}} \begin{pmatrix} \mathbf{I}_{(m-1)/2} & 0 & \mathbf{J}_{(m-1)/2} \\ 0 & \sqrt{2} & 0 \\ i \mathbf{I}_{(m-1)/2} & 0 & -i \mathbf{J}_{(m-1)/2} \end{pmatrix} & \text{for } m \text{ odd,} \end{cases} \quad (1)$$

then:

- $\mathbf{s} = \mathbf{T} \mathbf{p}$ is a real vector (if \mathbf{p} is centrosymmetric, i.e. $\mathbf{p} = \mathbf{J}_m \mathbf{p}^*$),
- $\mathbf{R} = \mathbf{T} \mathbf{M} \mathbf{T}^H$ is a real symmetric matrix.

Equivalent Detection Problem

Using previous transformation \mathbf{T} , the original problem can be reformulated as:

Original Problem	\mathbf{T}	Equivalent Problem
$\begin{cases} H_0 : \mathbf{y} = \mathbf{c}, & \mathbf{y}_k = \mathbf{c}_k, \\ H_1 : \mathbf{y} = A\mathbf{p} + \mathbf{c}, & \mathbf{y}_k = \mathbf{c}_k, \end{cases}$	\rightarrow	$\begin{cases} H_0 : \mathbf{z} = \mathbf{n}, & \mathbf{z}_k = \mathbf{n}_k, \\ H_1 : \mathbf{z} = A\mathbf{s} + \mathbf{n}, & \mathbf{z}_k = \mathbf{n}_k, \end{cases}$

where

- $\mathbf{z} = \mathbf{T}\mathbf{y} \in \mathbb{C}^m$,
- $\mathbf{n} = \sqrt{\tau}\mathbf{x}$ and $\mathbf{n}_k = \sqrt{\tau_k}\mathbf{x}_k$ with $\mathbf{x}, \mathbf{x}_k \sim \mathcal{CN}(\mathbf{0}, \mathbf{R})$ where \mathbf{R} is an unknown real symmetric matrix,
- $\mathbf{s} = \mathbf{T}\mathbf{p}$ is a real vector.

The main motivation for introducing the transformed data is that the original persymmetric covariance matrix of the Gaussian speckle \mathbf{M} is transformed into a real covariance matrix \mathbf{R} .

The Persymmetric FP Covariance Matrix Estimate

From the estimate $\hat{\mathbf{R}}_{FP}$ of the real covariance matrix \mathbf{R} , solution of the following equation:

$$\hat{\mathbf{R}} = \frac{m}{K} \sum_{k=1}^K \frac{\mathbf{n}_k \mathbf{n}_k^H}{\mathbf{n}_k^H \hat{\mathbf{R}}^{-1} \mathbf{n}_k},$$

the Persymmetric Fixed-Point Covariance Matrix Estimate can be defined as:

$$\hat{\mathbf{R}}_{PFP} = \mathcal{R}e(\hat{\mathbf{R}}_{FP}).$$

Statistical performance of $\hat{\mathbf{R}}_{PFP}$ [Pascal *et al.* 2008]:

- $\hat{\mathbf{R}}_{PFP}$ is a consistent estimate of \mathbf{R} when K tends to infinity,
- $\hat{\mathbf{R}}_{PFP}$ is an unbiased estimate of \mathbf{R} ,
- Its asymptotic distribution is the same as the asymptotic distribution of a real Wishart matrix with $\frac{m}{m+1} 2K$ degrees of freedom.

The Persymmetric Adaptive Normalized Matched Filter

The resulting P-ANMF for the transformed problem is based on the PFP estimate and can be defined as:

$$\Lambda(\hat{\mathbf{R}}_{PFP}) = \frac{|\mathbf{s}^\top \hat{\mathbf{R}}_{PFP}^{-1} \mathbf{z}|^2}{(\mathbf{s}^\top \hat{\mathbf{R}}_{PFP}^{-1} \mathbf{s})(\mathbf{z}^H \hat{\mathbf{R}}_{PFP}^{-1} \mathbf{z})} \underset{H_0}{\overset{H_1}{\geq}} \lambda. \quad (2)$$

Properties:

- $\Lambda(\hat{\mathbf{R}}_{PFP})$ is texture-CFAR,
- $\Lambda(\hat{\mathbf{R}}_{PFP})$ is matrix-CFAR,
- The use of PFP estimate in the ANMF allows to **virtually double the number K of secondary data** and improve the performance of the ANMF detector built with the FP matrix estimate.

$\Lambda(\hat{\mathbf{R}}_{PFP})$ is SIRV-CFAR and is called the P-ANMF.

Statistical study of the P-ANMF

$\Lambda(\hat{\mathbf{R}}_{PFP})$ has the same distribution as $\frac{F}{F+1}$ where

$$F = \frac{(\alpha_1 u_{22} - \alpha_2 u_{21})^2 + \left(1 + \left(\frac{\beta_3}{u_{33}}\right)^2\right) (a u_{22} - b u_{21})^2}{(\alpha_2 u_{11})^2 + \left(t_{11} u_{22} \frac{\beta_3}{u_{33}}\right)^2 + u_{11}^2 \left(1 + \left(\frac{\beta_3}{u_{33}}\right)^2\right) b^2} \quad (3)$$

and where: $a, b, \alpha_1, u_{21} \sim \mathcal{N}(0, 1)$, $\alpha_2^2 \sim \chi_{m-1}^2$, $\beta_3^2 \sim \chi_{m-2}^2$, $u_{11}^2 \sim \chi_{K'-m+1}^2$, $u_{22}^2 \sim \chi_{K'-m+2}^2$, $u_{33}^2 \sim \chi_{K'-m+3}^2$ with $K' = \frac{m}{m+1} 2K$.

Outline

1 More properties of the adaptive detectors

- Robustness of the M-estimators
- Adaptive Robust Detection in Clutter Transition
- Exploiting Prior Information: Covariance Structure
- Low Rank Detectors

2 Radar applications: Doppler detection/estimation, STAP

- Surveillance Radar Data
- OTH Radar Data
- STAP Data

3 Conclusions and Perspectives

Conventional Low Rank Detectors

Principle of Low Rank Matched Filter approaches found for example in [Kirstein *et al.*, 94] (Principal Component Inverse) and [Haimovich, 96] (Eigencanceler) and [Rangaswami *et al.*, 04].

Let suppose the rank r of clutter covariance matrix \mathbf{M} is known. For example, in the case of Space Time Adaptive Processing for airborne linear phased array radar acquiring M pulses with N sensors, this rank r is known (Brennan's rule) to be: $r = N + (M - 1) \beta$ where $\beta = 2 v T_r / d$ is the slope of the clutter ridge, T_r the Pulse Repetition Interval, v the platform velocity and d the inter-element spacing. The idea is to **project the data onto the orthogonal subspace of the clutter**. If we note

$$\hat{\mathbf{M}}_{SCM} = \frac{1}{K} \sum_{k=1}^K \mathbf{c}_k \mathbf{c}_k^H = (\mathbf{U}_r \mathbf{U}_0) \begin{pmatrix} \Sigma_r & \mathbf{0} \\ \mathbf{0} & \Sigma_0 \end{pmatrix} (\mathbf{U}_r \mathbf{U}_0)^H,$$

where \mathbf{U}_r and \mathbf{U}_0 are respectively two $(NM \times r)$ and $(NM \times NM - r)$ unitary matrices and Σ_r and Σ_0 are diagonal non-negative matrices. From low rank clutter assumption, we have the following eigenvalue property: $\lambda_1, \dots, \lambda_r \gg \lambda_{r+1}, \dots, \lambda_{NM}$. Therefore, we obtain the projector onto the clutter subspace $\Pi_{SCM} = \mathbf{U}_r \mathbf{U}_r^H$. We obtain the classical LR-ANMF-SCM:

$$\Lambda_{LR-ANMF-SCM}(\mathbf{y}) = \frac{|\mathbf{p}^H (\mathbf{I} - \Pi_{SCM}) \mathbf{y}|^2}{(\mathbf{p}^H (\mathbf{I} - \Pi_{SCM}) \mathbf{p})(\mathbf{z}^H (\mathbf{I} - \Pi_{SCM}) \mathbf{y})} \underset{H_0}{\overset{H_1}{\gtrless}} \lambda.$$

Extended Low Rank Detectors

In a case of heterogeneous and non-Gaussian clutter, we know that $\hat{\mathbf{M}}_{SCM}$ or Π_{SCM} are not good estimates. If we note the Normalized Sample Covariance Matrix as:

$$\mathbf{M}_{NSCM} = \frac{NM}{K} \sum_{k=1}^K \frac{\mathbf{c}_k \mathbf{c}_k^H}{\mathbf{c}_k^H \mathbf{c}_k} = (\mathbf{U}_r \mathbf{U}_0) \begin{pmatrix} \Sigma_r & \mathbf{0} \\ \mathbf{0} & \Sigma_0 \end{pmatrix} (\mathbf{U}_r \mathbf{U}_0)^H$$

where \mathbf{U}_r and \mathbf{U}_0 are respectively two $(NM \times r)$ and $(NM \times NM - r)$ unitary matrices and Σ_r and Σ_0 are diagonal non-negative matrices.

We can prove [Ginolhac *et al.*, 12] that $\Pi_{NSCM} = \mathbf{U}_r \mathbf{U}_r^H$ is a consistent estimate projector onto the clutter subspace.

Following the derivation found in the previous slide, we obtain the extended LR-ANMF-NSCM:

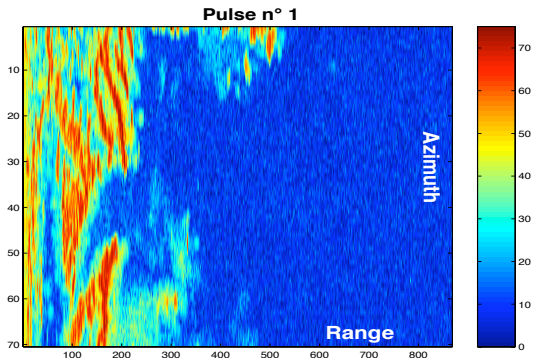
$$\Lambda_{LR-ANMF-NSCM}(\mathbf{y}) = \frac{|\mathbf{p}^H (\mathbf{I} - \Pi_{NSCM}) \mathbf{y}|^2}{(\mathbf{p}^H (\mathbf{I} - \Pi_{NSCM}) \mathbf{p})(\mathbf{z}^H (\mathbf{I} - \Pi_{NSCM}) \mathbf{y})} \underset{H_0}{\overset{H_1}{\gtrless}} \lambda.$$

This detector is found to be **texture-CFAR** and is **asymptotically M-CFAR**. Moreover, he has another nice **robustness property** when outliers and targets are present in the secondary data. The Normalized Sample Covariance Matrix is a good candidate for adaptive version of Rangaswami's Low Rank Matched Filter and Low Rank Normalized Matched Filter

Outline

- 1 More properties of the adaptive detectors
 - Robustness of the M-estimators
 - Adaptive Robust Detection in Clutter Transition
 - Exploiting Prior Information: Covariance Structure
 - Low Rank Detectors
- 2 Radar applications: Doppler detection/estimation, STAP
 - Surveillance Radar Data
 - OTH Radar Data
 - STAP Data
- 3 Conclusions and Perspectives

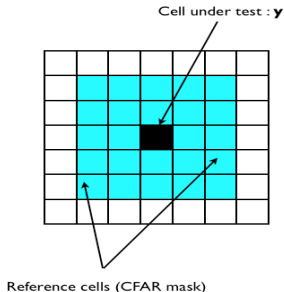
Data Description



- "Range-azimuth" map from ground clutter data collected by a radar from THALES Air Defence, placed 13 meters above ground and illuminating area at low grazing angle.
- Ground clutter complex echoes collected in 868 range bins for 70 different azimuth angles and for $m = 8$ pulses.

Data processing

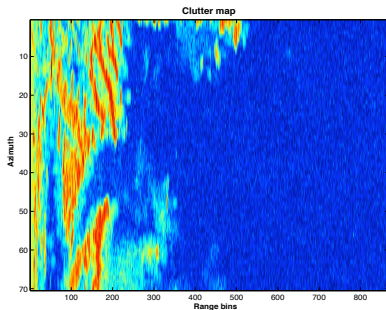
- Rectangular CFAR mask 5×5 for $0 \leq k \leq m$ different steering vectors \mathbf{p}_k .



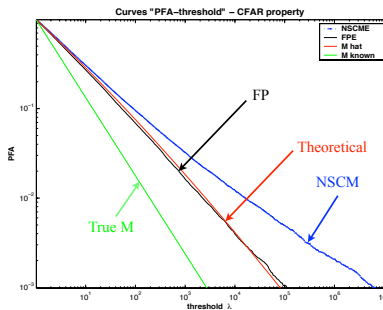
$$\mathbf{p}_k = \begin{pmatrix} 1 \\ \exp\left(\frac{2i\pi(k-1)}{m}\right) \\ \exp\left(\frac{2i\pi(k-1)2}{m}\right) \\ \vdots \\ \exp\left(\frac{2i\pi(k-1)(m-1)}{m}\right) \end{pmatrix}$$

- For each \mathbf{y} , computation of associated detectors $\Lambda_{ANMF}(\hat{\Sigma}_{Tyler})$ and $\Lambda_{ANMF}(\hat{\Sigma}_{NSCM})$
- Mask moving all over the map.

False Alarm Regulation Results on Experimental Data (Surveillance Radar)



Azimuth/range bins map

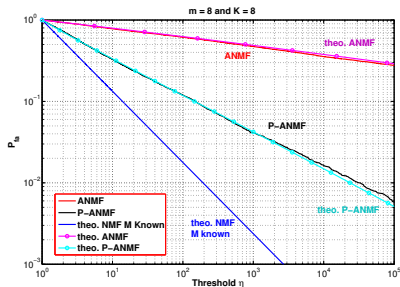


Relationship " P_{fa} -threshold"

Figure: False alarm regulation for $\mathbf{p}_0 = (1 \dots 1)^T$

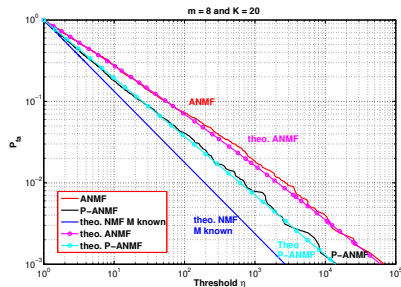
Black curve fits red curve until $PFA = 10^{-3}$!

False Alarm Regulation Results on Experimental Data



$K = 8$ (3×3 window)

limit of the invertibility of the matrix !!

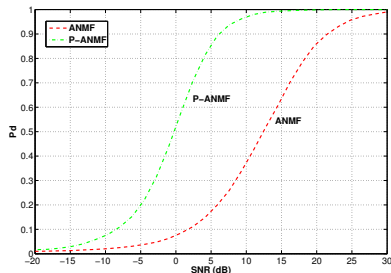


$K = 20$ (3×7 window)

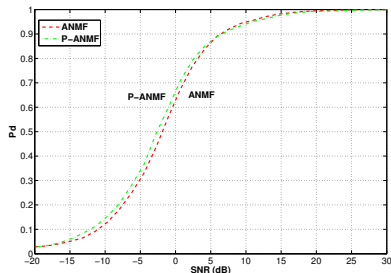
Figure: False alarm regulation for $\mathbf{p}_0 = (1 \dots 1)^T$

Black and Red curves fit blue and pink curves until $PFA = 10^{-3}$!

Detection Performance Results on Experimental Data



$$P_{fa} = 10^{-2}, m = 8, K = 8$$



$$P_{fa} = 10^{-2}, m = 8, K = 20$$

Figure: Probability of Detection for ANMF and P-ANMF

- for $K = m$, the P-ANMF outperforms the ANMF detection performance,
- for higher K ($K \gg m$), the P-ANMF and ANMF tend to have the same performance.

Outline

- 1 More properties of the adaptive detectors
 - Robustness of the M-estimators
 - Adaptive Robust Detection in Clutter Transition
 - Exploiting Prior Information: Covariance Structure
 - Low Rank Detectors
- 2 Radar applications: Doppler detection/estimation, STAP
 - Surveillance Radar Data
 - OTH Radar Data
 - STAP Data
- 3 Conclusions and Perspectives

False Alarm Regulation Results on Experimental Data (Nostradamus OTH)

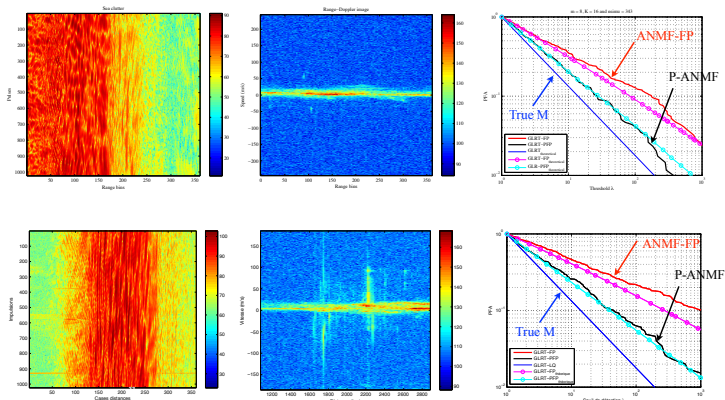
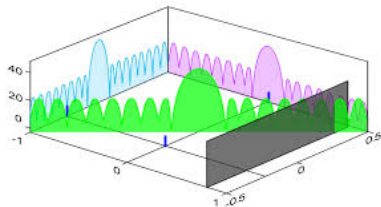


Figure: False Alarm Regulation for ANMF and P-ANMF over OTH experimental data: set of parameters: $m = 8$, $K = 13$, P_{fa} evaluation through 343 range profiles

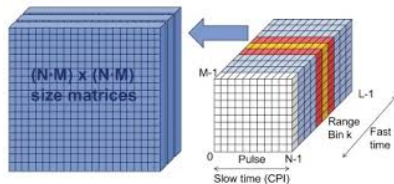
Outline

- 1 More properties of the adaptive detectors
 - Robustness of the M-estimators
 - Adaptive Robust Detection in Clutter Transition
 - Exploiting Prior Information: Covariance Structure
 - Low Rank Detectors
- 2 Radar applications: Doppler detection/estimation, STAP
 - Surveillance Radar Data
 - OTH Radar Data
 - STAP Data
- 3 Conclusions and Perspectives

Space Time Adaptive Processing: Principles



(a) STAP principles



(b) STAP datacube

$$\mathbf{p}(\theta, f_d) = \begin{pmatrix} 1 \\ \exp(-2i\pi d \sin(\theta)/\lambda) \\ \vdots \\ \exp(-2i\pi(N-1)d \sin(\theta)/\lambda) \end{pmatrix} \otimes \begin{pmatrix} 1 \\ \exp(-2i\pi f_d T_r) \\ \vdots \\ \exp(-2i\pi f_d (M-1) T_r) \end{pmatrix}$$

STAP Principles

Problem: estimate the position (angle) and the Doppler frequency (speed) of the target \Rightarrow use of the ANMF with a particular steering vector

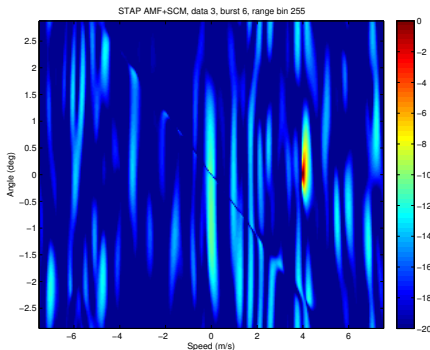
Data parameters: real clutter with synthetic target

X-Band $\simeq 10^9$ Hz, wavelength $\lambda = 0.03\text{m}$, flight speed $v = 100\text{m/s}$, distance to the scene 30km, 5 deg of incidence, PRF (Pulse Repetition Frequency) of 1 kHz, inter-sensor distance $d = 0.3\text{m}$, 12 trials with $K = 410$ range bins, $M = 64$ pulses and $N = 4$ sensors.

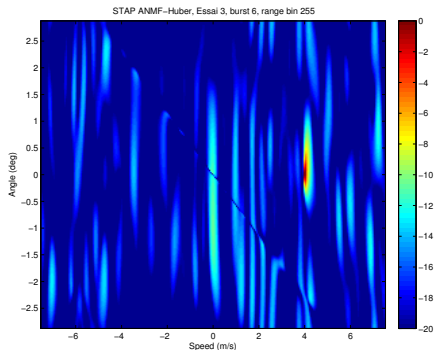
This means observations of size $m = 256$ while $K \leq 410$!

Clutter more or less homogeneous **BUT** targets are present in the secondary data

No target is present in the secondary data - homogeneous noise



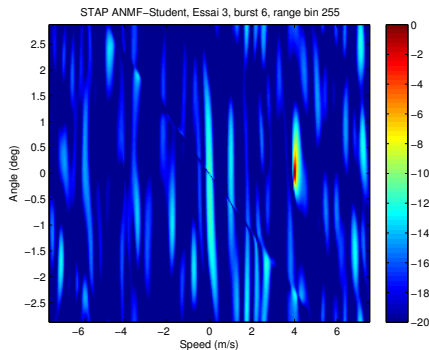
(c) AMF detector with the SCM



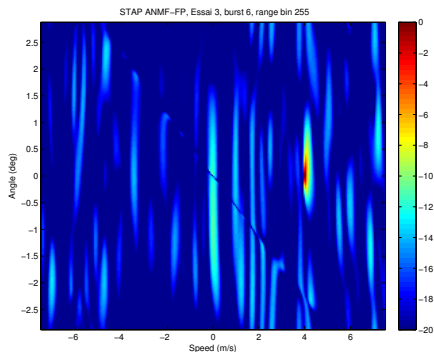
(d) ANMF detector with Huber's est. (parameter $q = 0.6$)

Figure: Doppler-angle map for the range bin 255 with $K = 404$ secondary data (targets and guard cells are removed) and $m = 256$

No target is present in the secondary data - homogeneous noise



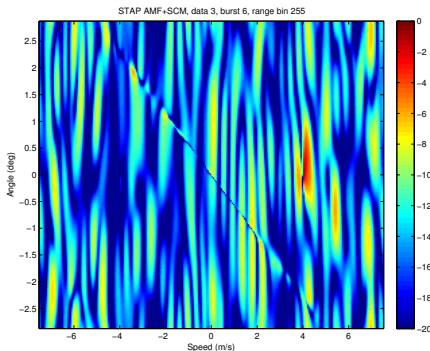
(a) ANMF detector with the Student est.
(parameter $\nu = 2$)



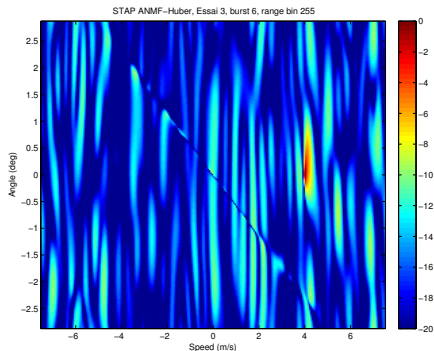
(b) ANMF detector with Tyler's est.

Figure: Doppler-angle map for the range bin 255 with $K = 404$ secondary data (targets and guard cells are removed) and $m = 256$

Two targets (4m/s and -4m/s) are present in the secondary data -
homogeneous noise



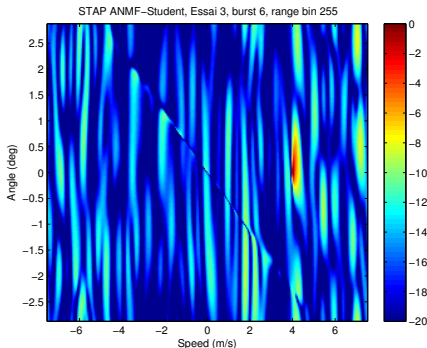
(a) AMF detector with the SCM



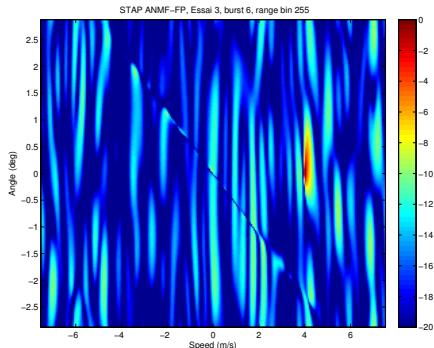
(b) ANMF detector with Huber's est. (parameter $q = 0.6$)

Figure: Doppler-angle map for the range bin 255 with $K = 404$ secondary data (guard cells are removed) and $m = 256$

Two targets (4m/s and -4m/s) are present in the secondary data -
homogeneous noise



(a) ANMF detector with the Student est.
(parameter $\nu = 2$)



(b) ANMF detector with Tyler's est.

Figure: Doppler-angle map for the range bin 255 with $K = 404$ secondary data
(guard cells are removed) and $m = 256$

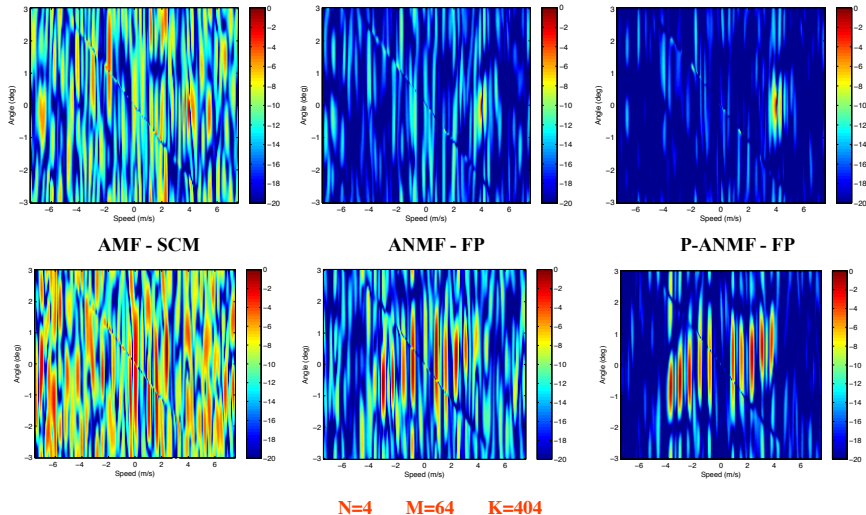


Figure: Doppler-angle map for the range bin 255 with $K = 404$ secondary data (guard cells are removed) and $m = 256$

No target-contamination, Target at 4 m/s, 0 deg

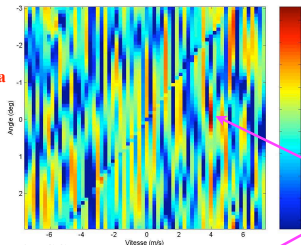
AMF based based on the SCM

Only one target detection

Non contaminated secondary data

$N=4$ $M=64$ $K=408$

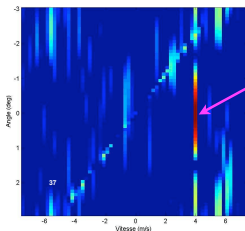
$K < 2MN$, $K > 2r$



Classical STAP

Target in the CUT

Low Rank AMF with SCM



Low Rank ANMF with NSCM

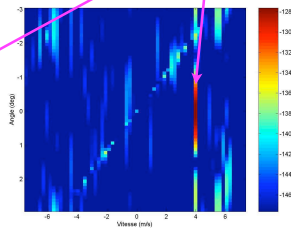


Figure: Doppler-angle map for the range bin 255 with $K = 408$ secondary data (guard cells are removed) and $m = 256$

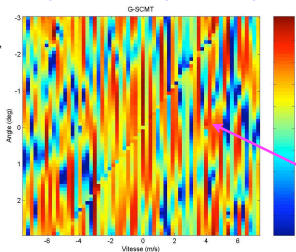
Only one target (4m/s) in the CUT

Contaminated secondary data
 (two targets at 4m/s and -4m/s)

$N=4$ $M=64$ $K=410$

$K < 2MN$, $K > 2r$

Target-contamination, Target at 4 m/s, 0 deg

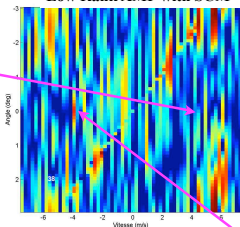


Classical STAP

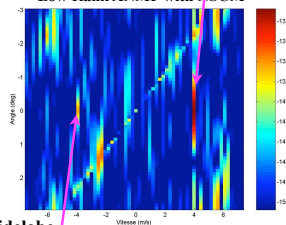
Target in the CUT

Low Rank AMF with SCM

Whitened target



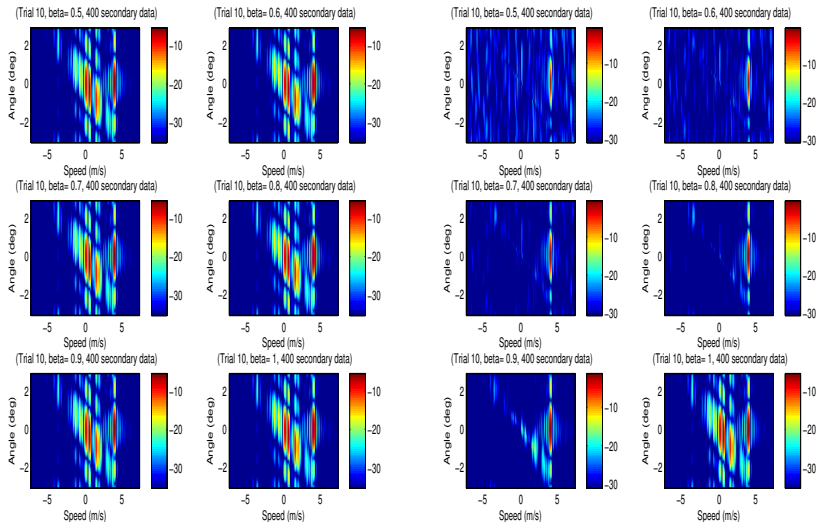
Low Rank ANMF with NSCM



Target sidelobe

Figure: Doppler-angle map for the range bin 255 with $K = 410$ secondary data (guard cells are removed) and $m = 256$

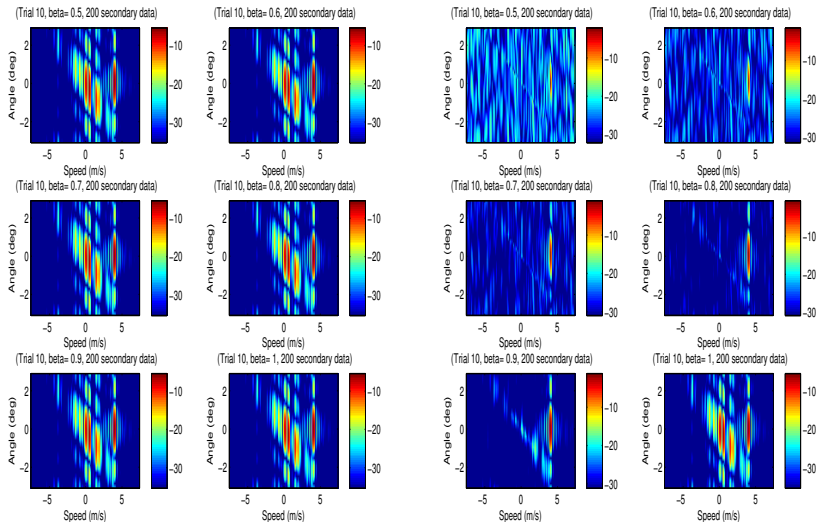
Applications to STAP data for \neq values of β . $m = 256$ and $K = 400$



(a) SCM

(b) Shrinkage FPE

Applications to STAP data for \neq values of β . $m = 256$ and $K = 200 \leq m$



(c) SCM

(d) Shrinkage FPE

Outline

- 1 More properties of the adaptive detectors
 - Robustness of the M-estimators
 - Adaptive Robust Detection in Clutter Transition
 - Exploiting Prior Information: Covariance Structure
 - Low Rank Detectors
- 2 Radar applications: Doppler detection/estimation, STAP
 - Surveillance Radar Data
 - OTH Radar Data
 - STAP Data
- 3 Conclusions and Perspectives

Conclusions

When the clutter is non-Gaussian and/or heterogeneous, the conventional detectors (AMF or sub-optimal CFAR tests) are not at all optimal and lead to poor false alarm regulation and poor detection performance,

The SIRV and CES clutter model allows to take into account the clutter complexity: the non-Gaussianity, the temporal clutter fluctuations and the spatial clutter power fluctuations,

Using this model, the ANMF detector built with the Fixed Point (or other \mathbf{M} -estimators) clutter covariance matrix estimator is shown to be CFAR-texture, CFAR-matrix and exhibits nice properties (robustness) and very good detection performance,

Conclusions

Taking into account additional a priori properties on the covariance matrix structure (low rank, persymmetry, Toeplitz, ...) can lead to a appreciable gain for small numbers of secondary data,

These methods can be applied for many problems involving covariance matrix estimation: STAP detection, SAR detection (FOPEN), Polarimetric/Interferometric SAR detection and classification, SAR Change Detection, Hyperspectral Anomaly detection, Hyperspectral detection.

Perspectives

Link with **Random Matrix Theory**: for high dimensionality data (ex: hyperspectral, STAP), strong statistical connexion with Robust Estimation theory [F. Pascal, R. Couillet, ...],

Low-rank detection with **M-Estimators** [G. Ginolhac, F. Pascal, A. Breloy],

Joint location and scale with **M-Estimators** (non-centered multivariate data, e.g. hyperspectral data),

Shrinkage of **M-Estimators** [A. Wiesel, Y. Abramovitch, O. Besson, F. Pascal, ...],

References and other applications

There have been other applications for CES distributions and robust estimators...

One can cite:

- Multivariate SAR imaging

G. Vasile, J-P. Ovarlez, F. Pascal and C. Tison, "Coherency Matrix Estimation of Heterogeneous Clutter in High-Resolution Polarimetric SAR Images," *Geoscience and Remote Sensing, IEEE Transactions on*, vol. 48, pp. 1809-1826, 2010.

- Image processing

F. Pascal, L. Bombrun, J.-Y. Tournet and Y. Berthoumieu, "Parameter Estimation for Multivariate Generalized Gaussian Distributions," *Signal Processing, IEEE Transactions on*, vol. 61, no. 23, pp. 5960-5971, 2013.

- Hyperspectral Detection

J. Frontera-Pons, J.P. Ovarlez, F. Pascal, "Robust Anomaly Detection and Detection in Hyperspectral Images", IGARSS Conference 2011-2014, IEEE CAMSAP 2011, IEEE Trans. on SP and GRS (on review)

Acknowledgements

- Philippe Forster, ENS Cachan, France
- Guillaume Ginolhac, Annecy University, France
- Pascal Larzabal, ENS Cachan, France

References

Many references relative to this tutorial (as well as updated version of this tutorial) can be found on my homepage:

<http://www.jeanphilippeovarlez.com>